A Synthetic, Structural, Magnetic, and Spectral Study of Several {Fe[tris(pyrazolyl)methane]$_2$}(BF$_4$)$_2$ Complexes: Observation of an Unusual Spin-State Crossover

Daniel L. Reger* and Christine A. Little

Department of Chemistry and Biochemistry, University of South Carolina, Columbia, South Carolina 29208

Arnold L. Rheingold, Matthew Lam, Louise M. Liable-Sands, Brian Rhagitan, and Tom Concolino

Department of Chemistry and Biochemistry, University of Delaware, Newark, Delaware 19716

Amitabh Mohan and Gary J. Long*

Department of Chemistry, University of Missouri—Rolla, Rolla, Missouri 65409-0010

Valérie Briois

Laboratoire pour l'Utilisation du Rayonnement Electromagnétique, Université de Paris Sud, F-91405 Orsay, France

Fernande Grandjean

Institut de Physique, B5, Université de Liège, B-4000 Sart-Tilman, Belgium

Received October 3, 2000

The complexes {Fe[HC(3,5-Me$_2$pz)$_3$]$_2$}(BF$_4$)$_2$ (**1**), {Fe[HC(pz)$_3$]$_2$}(BF$_4$)$_2$ (**2**), and {Fe[PhC(pz)$_2$(py)]$_2$}(BF$_4$)$_2$ (**3**) (pz = 1-pyrazolyl ring, py = pyridyl ring) have been synthesized by the reaction of the appropriate ligand with Fe(BF$_4$)$_2$·6H$_2$O. Complex **1** is high-spin in the solid state and in solution at 298 K. In the solid phase, it undergoes a decrease in magnetic moment at lower temperatures, changing at ca. 206 K to a mixture of high-spin and low-spin forms, a spin-state mixture that does not change upon subsequent cooling to 5 K. Crystallographically, there is only one iron(II) site in the ambient-temperature solid-state structure, a structure that clearly shows the complex is high-spin. Mössbauer spectral studies show conclusively that the magnetic moment change observed at lower temperatures arises from the complex changing from a high-spin state at higher temperatures to a 50:50 mixture of high-spin and low-spin states at lower temperatures. Complexes **2** and **3** are low-spin in the solid phase at room temperature. Complex **2** in the solid phase gradually changes over to the high-spin state upon heating above 295 K and is completely high-spin at ca. 470 K. In solution, variable-temperature ^{1}H NMR spectra of **2** show both high-spin and low-spin forms are present, with the percentage of the paramagnetic form increasing as the temperature increases. Complex **3** is low-spin at all temperatures studied in both the solid phase and solution. An X-ray absorption spectral study has been undertaken to investigate the electronic spin states of {Fe[HC(3,5-Me$_2$pz)$_3$]$_2$}(BF$_4$)$_2$ and {Fe[HC(pz)$_3$]$_2$}(BF$_4$)$_2$. Crystallographic information: **2** is monoclinic, $P2_1/n$, a = 10.1891(2) Å, b = 7.6223(2) Å, c = 17.2411(4) Å, β = 100.7733(12)°, Z = 2; **3** is triclinic, $P\bar{1}$, a = 12.4769(2) Å, b = 12.7449(2) Å, c = 13.0215(2) Å, α = 83.0105(8)°, β = 84.5554(7)°, γ = 62.5797(2)°, Z = 2.

Introduction

The pseudooctahedral coordination complexes of iron(II) provide the classic examples of the high-spin (HS), low-spin (LS), and spin-transition or spin-crossover complexes for the 3d^6 electronic configuration.[1] In an octahedral iron(II) complex, below a critical crystal field, the iron has the $t_{2g}^4e_g^2$, $^5T_{2g}$, high-spin ground-state electronic configuration, whereas above this field it has the t_{2g}^6, $^1A_{1g}$, low-spin ground-state electronic configuration. If the crystal field experienced by the iron(II) is similar to the critical field, the complex may show a spin-state transformation between the two spin states,[1] usually a spin-state crossover for iron(II) complexes. In general, iron(II) complexes which are HS in the solid state at room temperature may show

(1) (a) Gütlich, P. In *Mössbauer Spectroscopy Applied to Inorganic Chemistry*; Long, G. J., Ed.; Plenum: New York, 1984; Vol. 1, p 287. (b) Gütlich, P.; Hauser, A.; Spiering, H. *Angew. Chem., Int. Ed. Engl.* **1994**, *33*, 2024. (c) Cotton, F. A.; Wilkinson, J.; Murillo, C. A.; Bochmann, M. *Advanced Inorganic Chemistry*, 6th ed.; John Wiley & Sons: New York, 1999; pp 785−786.

10.1021/ic001102t CCC: $20.00
Published on Web 02/17/2001

Chart 1

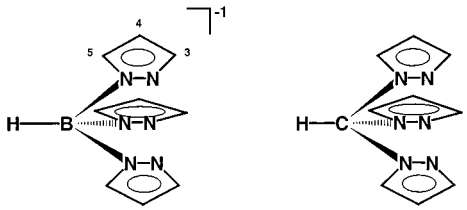

a spin crossover to the LS electronic state upon cooling, whereas complexes which are LS at room temperature may show a spin crossover to the HS electronic state upon heating.[2−4]

Coordination complexes containing various substituted tris(pyrazolyl)borate ligands[5] (Chart 1) have been very useful in investigating the spin-state transitions in transition-metal complexes. The complexes Fe[HB(pz)$_3$]$_2$, Fe[HB(3,5-Me$_2$pz)$_3$]$_2$, and Fe[HB(3,4,5-Me$_3$pz)$_3$]$_2$ (pz = 1-pyrazolyl ring) have been the subject of several Mössbauer spectral studies as a function of temperature.[2,3] The room-temperature single-crystal X-ray structure of Fe[HB(pz)$_3$]$_2$ shows Fe−N bond distances of 1.97 Å,[6] typical of LS octahedral complexes.[1] In the structure of Fe[HB(3,5-Me$_2$pz)$_3$]$_2$ at 295 K, the Fe−N bond distances are 2.17 Å,[6] a value which is typical of the HS state.[1] Thus, the spin-state change is responsible for a 10% change in the average Fe−N distance. Upon a change in temperature, these three complexes yield different spin-state behaviors. A variety of techniques[2,7] indicate that Fe[HB(pz)$_3$]$_2$ is LS below 400 K and exhibits a gradual change to the HS state above 400 K. In contrast, Fe[HB(3,5-Me$_2$pz)$_3$]$_2$ shows[3] a relatively sharp spin-state crossover from HS above 195 K to LS below 195 K, whereas Fe[HB(3,4,5-Me$_3$pz)$_3$]$_2$ is HS at 293 K and shows[2b] no spin crossover upon cooling to 1.7 K.

Some of us have recently been exploring the coordination chemistry of the tris(pyrazolyl)methane family of ligands (Chart 1).[8] One of the goals of this research is to compare the chemistry of these neutral ligands with the more extensively studied isoelectronic, but anionic, tris(pyrazolyl)borate ligands. In the chemistry of cadmium(II), the two ligand types seem to behave in a very similar fashion. For example, the isoelectronic pair Cd[HB(3,5-Me$_2$pz)$_3$]$_2$ and {Cd[HC(3,5-Me$_2$pz)$_3$]$_2$}$^{2+}$ have nearly the same Cd−N bond distances of 2.348(5) and 2.321(10) Å, respectively, and nearly the same ^{113}Cd NMR chemical shifts of 202 and 207 ppm, respectively.[8b]

As part of our program to develop the chemistry of the tris(pyrazolyl)methane ligands, we decided to prepare {Fe[tris(pyrazolyl)methane]$_2$}$^{2+}$ complexes and compare their properties to the tris(pyrazolyl)borate analogues. We anticipated that the spin-state behavior of the complexes could be controlled by changes in substituents on the ligands and changes in the counterions. Prior to our work, the synthesis and visual absorption and Mössbauer spectral results on {Fe[HC(pz)$_3$]$_2$}$^{2+}$ had been reported,[9] and after completion of our work, a structural study of two forms of {Fe[HC(pz)$_3$]$_2$}(NO$_3$)$_2$ was reported.[10]

Herein we report the synthetic, structural, magnetic, and NMR, Mössbauer, and X-ray absorption spectral results for {Fe[HC(3,5-Me$_2$pz)$_3$]$_2$}(BF$_4$)$_2$ (**1**), {Fe[HC(pz)$_3$]$_2$}(BF$_4$)$_2$ (**2**), and {Fe[PhC(pz)$_2$(py)]$_2$}(BF$_4$)$_2$ (**3**) (py = pyridyl ring). Complex **1** is HS at room temperature, but shows a very unusual thermally induced change in its spin state at lower temperatures. The latter two complexes are LS at room temperature, with **2** gradually changing over to HS above room temperature. We have communicated preliminary results on **1** previously.[11]

Experimental Section

General Procedure. All operations were carried out under a nitrogen atmosphere either using standard Schlenk techniques or in a Vacuum Atmospheres HE-493 drybox. All solvents were dried and distilled prior to use. Proton NMR chemical shifts are reported in parts per million versus TMS. HC(3,5-Me$_2$pz)$_3$, HC(pz)$_3$ and PhC(pz)$_2$(py) were prepared according to our recently reported procedures.[12] Elemental analyses were performed by National Chemical Consulting, Inc. and Robertson Microlit Laboratories, Inc.

Magnetic susceptibilities were measured at 5 kG using a Quantum Design MPMS XL SQUID magnetometer. Clear gelatin capsules were used as sample containers for measurements taken in the temperature range 5−400 K. The very small diamagnetic contribution of the gelatin capsule had a negligible contribution to the overall magnetization, which was dominated by the sample. The high-temperature data (400−600 K) were collected with a sample space oven installed on the SQUID magnetometer using a brass sample holder.

{Fe[HC(3,5-Me$_2$pz)$_3$]$_2$}(BF$_4$)$_2$ (1). A THF solution (10 mL) of Fe(BF$_4$)$_2$·6H$_2$O (0.68 g, 2.0 mmol) was treated dropwise by cannula transfer with a THF solution (20 mL) of HC(3,5-Me$_2$pz)$_3$ (1.50 g, 5.03 mmol). The reaction mixture was stirred overnight, yielding a white solid. The liquid was removed by cannula filtration, and the remaining white solid was washed with hexanes (3 × 10 mL) and dried under vacuum (1.41 g, 85%). The crystals used for magnetic, X-ray crystallographic, and Mössbauer spectral studies were grown by layering

(2) (a) Grandjean, F.; Long, G. J.; Hutchinson, B. B.; Ohlhausen, L.; Neill, P.; Holcomb, J. D. *Inorg. Chem.* **1989**, *28*, 4406. (b) Long, G. J.; Hutchinson, B. B. *Inorg. Chem.* **1987**, *26*, 608.
(3) (a) Jesson, J. P.; Trofimenko, S.; Eaton, D. R. *J. Am. Chem. Soc.* **1967**, *89*, 3158. (b) Jesson, J. P.; Weiher, J. F.; Trofimenko, S. *J. Chem. Phys.* **1968**, *48*, 2058.
(4) (a) Cartier dit Moulin, C.; Rudolf, P.; Flank, A.-M.; Chen, C.-T. *J. Phys. Chem.* **1992**, *96*, 6196. (b) Cartier dit Moulin, C.; Sainctavit, P.; Briois V. *Jpn. J. Appl. Phys.* **1993**, *32* (Suppl. 32-2), 38. (c) Briois, V.; Cartier dit Moulin, C.; Momenteau, M.; Maillard, P.; Zarembowitch, J.; Dartyge, E.; Fontaine, A.; Tourillon, G.; Thuéry, P.; Verdaguer, M. *J. Chim. Phys. Phys.-Chim. Biol.* **1989**, *86*, 1623. (d) Young, N. A. *J. Chem. Soc., Dalton Trans.* **1996**, 1275. (e) Real, J.-A.; Gallois, B.; Granier, T.; Suez-Panama, F.; Zarembowitch, J. *Inorg. Chem.* **1992**, *31*, 4972. (f) Breuning, E.; Ruben, M.; Lehn, J.-L.; Renz, F.; Garcia, Y.; Ksenofonyov, V.; Gütlich, P.; Wegelius, E.; Rissanen, K. *Angew. Chem., Int. Ed.* **2000**, *39*, 2504.
(5) (a) Trofimenko, S. *Scorpionates—The Coordination Chemistry of Poly(pyrazolyl)borate Ligands*; Imperial College Press: London, 1999. (b) Trofimenko, S. *Chem. Rev.* **1993**, *93*, 943.
(6) Oliver, J. D.; Mullica, D. F.; Hutchinson, B. B.; Milligan, W. O. *Inorg. Chem.* **1980**, *19*, 165.
(7) Bruno, G.; Centineo, G.; Ciliberto, E.; Di Bella, S.; Fragala, I. *Inorg. Chem.* **1984**, *23*, 1832.
(8) (a) Reger, D. L. *Comments Inorg. Chem.* **1999**, *21*, 1. (b) Reger, D. L.; Collins, J. E.; Myers, S. M.; Rheingold, A. L.; Liable-Sands, L. M. *Inorg. Chem.* **1996**, *35*, 4904. (c) Reger, D. L.; Collins, J. E.; Rheingold, A. L.; Liable-Sands, L. M.; Yap, G. P. A. *Inorg. Chem.* **1997**, *36*, 345. (d) Reger, D. L.; Collins, J. E.; Jameson, D. L.; Castellano, R. K. *Inorg. Synth.* **1998**, *32*, 63. (e) Reger, D. L. Collins, J. E.; Rheingold, A. L.; Liable-Sands, L. M. *Organometallics* **1996**, *15*, 2029. (f) Reger, D. L.; Collins, J. E.; Rheingold, A. L.; Liable-Sands, L. M.; Yap, G. P. A. *Organometallics* **1997**, *16*, 349. (g) Reger, D. L.; Collins, J. E.; Layland, R.; Adams, R. D. *Inorg. Chem.* **1996**, *35*, 1372. (h) Reger, D. L.; Collins, J. E.; Rheingold, A. L.; Liable-Sands, L. M. *Inorg. Chem.* **1999**, *38*, 3235. (i) Reger, D. L.; Collins, J. E.; Mathews, M. A.; Rheingold, A. L.; Liable-Sands, L. M.; Guzei, I. A. *Inorg. Chem.* **1997**, *36*, 6266.
(9) (a) McGarvey, J. J.; Toftlund, H.; Al-Obaidi, A. H. R.; Taylor, K. P.; Bell, S. E. J. *Inorg. Chem.* **1993**, *32*, 2469. (b) Winkler, H.; Trautwein, A. X.; Toftlund, H. *Hyperfine Interact.* **1992**, *70*, 1083. (c) Mani, F. *Inorg. Nucl. Chem. Lett.* **1979**, *15*, 297.
(10) Anderson, P. A.; Astley, T.; Hitchman, M. A.; Keene, F. R.; Moubaraki, B.; Murray, K. S.; Skelton, B. W.; Tiekink, E. R. T.; Toftlund, H.; White, A. H. *J. Chem. Soc., Dalton Trans.* **2000**, 3505.
(11) Reger, D. L.; Little, C. A.; Rheingold, A L.; Lam, K.-C.; Concolino, T.; Mohan, A.; Long, G. J. *Inorg. Chem.* **2000**, *39*, 4674.
(12) Reger, D. L.; Grattan, T. C.: Brown, K. J.; Little, C. A.; Lamba, J. J. S.; Rheingold, A L.; Sommer, R D. *J. Organomet. Chem.* **2000**, *607*, 120.

a saturated acetone solution with hexanes and allowing the two layers to slowly combine; dec above 335 °C. In this preparation, use of $Fe(BF_4)_2 \cdot 6H_2O$ from a bottle that has previously been opened in the air leads to the formation of variable amounts of $\{Fe[HC(3,5\text{-}Me_2pz)_3](H_2O)_3\}(BF_4)_2$[13] in addition to the desired **1**. Even in those reactions that successfully yield only **1**, some of the less soluble $\{Fe[HC(3,5\text{-}Me_2pz)_3](H_2O)_3\}(BF_4)_2$ precipitates initially, but it reacts with additional ligand over the course of the reaction to yield the desired complex. If **1** is contaminated with the aqua complex, the mixture can be treated with additional ligand to yield pure complex **1**. ^{1}H NMR (acetone-d_6, 293 K): δ 51.8 (6, v br, 4-*H* (pz)), 41.2, 19.8 (18, 18, v br, v br, Me_2), −42.3 (2, v br, *H*C). ^{1}H NMR (acetone-d_6, 185 K): δ 80.5 (6, v br, 4-*H* (pz)), 72.6, 26.0 (18, 18, v br, v br, Me_2), −82.7 (2, v br, *H*C). FAB^+ MS: *m*/*z* calcd for $\{Fe[HC(3,5\text{-}Me_2pz)_3]_2\}(BF_4)^+$ 739.3190, found 739.3168.

$\{Fe[HC(pz)_3]_2\}(BF_4)_2$ (2). A THF solution (10 mL) of $Fe(BF_4)_2 \cdot 6H_2O$ (0.26 g, 0.77 mmol) was treated dropwise by cannula transfer with a THF (10 mL) solution of $HC(pz)_3$ (0.34 g, 1.6 mmol). A purple solid precipitated immediately from the solution. The reaction mixture was allowed to stir for 30 min before cannula filtration. The remaining purple solid was washed with diethyl ether (3 × 10 mL) and dried under vacuum (0.42 g, 84%). The crystals used for magnetic, X-ray crystallographic, and Mössbauer spectral studies were grown by layering benzene with a saturated acetonitrile solution and allowing the two layers to slowly combine; dec above 345 °C. ^{1}H NMR (dmf-d_7, 293 K): (paramagnetic resonances) δ 46.6, 46.6,16.3 (6, 6, 6, pz), −32.3 (2, *H*C); (diamagnetic resonances) δ 9.30 (2, s, *H*C), 9.00, 8.69 (6, 6, s, s, 3,5-*H* (pz)), 7.65 (6, s, 4-*H* (pz)). Anal. Calcd for $C_{20}H_{20}N_{12}FeB_2F_8$: C, 36.51, H, 3.06. Found: C, 36.57, H, 3.18. FAB^+ MS: *m*/*z* calcd for $\{Fe[HC(pz)_3]_2\}(BF_4)^+$ 571.1312, found 571.1323.

$\{Fe[PhC(pz)_2(py)]_2\}(BF_4)_2$ (3). A THF solution (10 mL) of $Fe(BF_4)_2 \cdot 6H_2O$ (0.20 g, 0.59 mmol) was treated dropwise by cannula transfer with a THF (10 mL) solution of $PhC(pz)_2(py)$ (0.36 g, 1.2 mmol). A dark red solid precipitated immediately from the solution. The reaction mixture was allowed to stir for 30 min before cannula filtration. The remaining red solid was washed with diethyl ether (3 × 10 mL) and dried under vacuum (0.46 g, 93%). Crystals suitable for an X-ray crystallographic and Mössbauer spectral study were grown by layering a saturated acetone solution with hexanes and allowing the two layers to slowly combine; dec above 236 °C. ^{1}H NMR (acetone-d_6, individual resonances could not be assigned due to the complexity of the spectrum): complex resonances centered at δ 8.51, 8.41, 8.26, 8.18, 7.99, 7.85, 7.61, 7.58, 7.52, 7.49, 6.72. Anal. Calcd for $C_{36}H_{30}N_{10}FeB_2F_8$: C, 51.96, H, 3.63. Found: C, 52.02, H, 3.23.

Mössbauer Spectral Data. The Mössbauer spectral absorbers contained 60 mg/cm^2 of powder, and the spectra were measured between 4.2 and 472 K on a constant-acceleration spectrometer which utilized a room-temperature rhodium matrix cobalt-57 source and was calibrated at room temperature with α-iron foil. The estimated absolute errors are ±0.01 mm/s for the isomer shifts, ±0.02 mm/s for the quadrupole splittings, and ±0.5% for the relative areas of the high-spin and low-spin spectral components. The relative errors are estimated to be smaller by a factor of 5−10.

X-ray Absorption Spectral Data. The X-ray absorption spectra were recorded with the synchrotron radiation provided by the DCI storage ring at the Laboratoire pour l'Utilisation du Rayonnement Electromagnétique, Université de Paris Sud, France. The synchrotron radiation was produced by a storage ring operated with 1.85 GeV positrons and with a current intensity of ca. 200 mA. The 295 and 78 K measurements were performed with the EXAFS III spectrometer, which uses a double-crystal silicon(311) monochromator. The measurements were carried out in the transmission mode with ionization chambers in front of and behind the absorber. Absorbers containing 25 mg/cm^2 of sample were used for both the XANES and EXAFS studies. The XANES spectra were recorded with a 0.25 eV step over a 125 eV energy range. The EXAFS spectra were recorded with a 2 eV step and with a 1 s accumulation time per step over a 1000 eV energy range. The spectrum of iron foil was recorded periodically to check the energy calibration, and the first derivative of the iron foil K-edge spectrum at 7112 eV was used to define the zero energy reference point.

X-ray Structural Data. Crystal, data collection, and refinement parameters are given in Table 1. The systematic absences in the diffraction data for **1** are consistent with the space groups *Cc* and *C*2/*c*. For **3**, there is no evidence of symmetry higher than triclinic. *E*-statistics and the presence of an inversion center for the cationic iron(II) complexes suggest the centrosymmetric space group *C*2/*c* for **1** and $P\bar{1}$ for **3**, space groups which yield chemically reasonable and computationally stable refinements. The systematic absences in the diffraction data for **2** are uniquely consistent with the reported $P2_1/n$ space group. The structures were solved using direct methods, completed by subsequent difference Fourier syntheses, and refined by full-matrix least-squares procedures. SADABS absorption corrections were applied to all data sets. In structures **1** and **2** the asymmetric unit contains half the cationic iron(II) complex, which lies on an inversion center, and one of the respective anions. The asymmetric unit of **3** contains two half cationic iron(II) complexes that lie on inversion centers, half an acetone molecule that is disordered over an inversion center, and two positionally disordered BF_4^- counterions. The pyridyl ring is compositionally disordered with one of the pyrazolyl rings in one of the cations, in which the atoms N(11′), N(12′), C(11′), C(12′), C(12A), C(12B), and C(13′) were refined as a pyrazolyl ring and the atoms N(21′), C(21′), C(22′), C(23′), C(24′), and C(25′) were refined as a pyridyl ring. All non-hydrogen atoms were refined with anisotropic displacement coefficients. In structures **1** and **2**, the hydrogen atom of C(30) was located from the difference map and its position was refined; all other hydrogen atoms were treated as idealized contributions. The hydrogen atoms of the disordered pyridyl/pyrazolyl rings and the acetone molecule of **3** were ignored. All software and sources of the scattering factors are contained in the SHELXTL (5.10) program library (G. Sheldrick, Siemens XRD, Madison, WI).

Results and Discussion

Syntheses of the Complexes. The reaction of $Fe(BF_4)_2 \cdot 6H_2O$ and $HC(3,5\text{-}Me_2pz)_3$ in a 1:2.5 ratio yields **1**. The solid is white as a powder and colorless as single crystals, indicating that the iron(II) is HS at room temperature.[1,14]

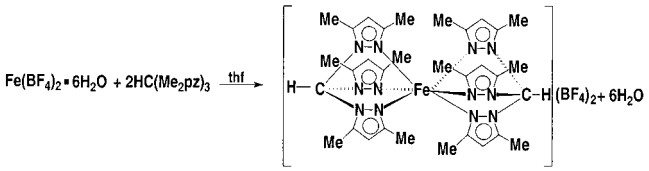

1

The reaction of $Fe(BF_4)_2 \cdot 6H_2O$ and $HC(pz)_3$ in a 1:2 ratio in THF leads to the immediate precipitation of **2**. This complex is purple at ambient temperatures, indicating that the iron(II) is in a LS state. It is not soluble in common organic solvents, although it does partially dissolve in acetonitrile and dissolves in dimethylformamide (DMF).

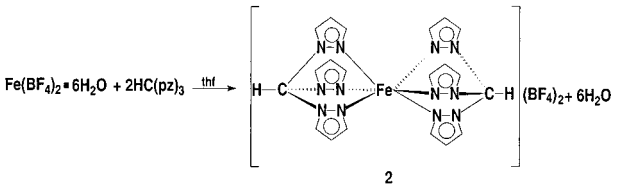

2

The reaction of $Fe(BF_4)_2 \cdot 6H_2O$ and $PhC(pz)_2(py)$ in a 1:2 ratio in THF leads to the immediate precipitation of **3**. This complex is red and has a "normal" diamagnetic NMR spectrum at room temperature, indicating that it is LS at this temperature.

(13) Reger, D. L.; Little, C. A.; Rheingold, A L.; Sommer, R. D.; Long, G. J. *Inorg. Chim. Acta*, in press.

(14) Kahn, O.; Martinez, J. *Science* **1998**, *279*, 44.

Table 1. Crystallographic Data for the Structural Analyses of **1**−**3**

	1	**2**	**3**
empirical formula	$C_{32}H_{44}B_2F_8FeN_{12}$	$C_{20}H_{20}B_2F_8FeN_{12}$	$C_{37.5}H_{33}B_2F_8FeN_{10}O_{0.5}$
fw	826.3	657.95	861.21
space group	*C*2/*c*	$P2_1/n$	$P\bar{1}$
a, Å	20.4992(4)	10.1891(2)	12.4769(2)
b, Å	10.4040(2)	7.6223(2)	12.7449(2)
c, Å	19.8147(4)	17.2411(4)	13.0215(2)
α, deg	90	90	83.0105(8)
β, deg	111.32289(12)	100.7733(12)	84.5554(7)
χ, deg	90	90	62.5797(2)
radiation (λ = 0.71073 Å)	Mo Kα	Mo Kα	Mo Kα
V, Å^3	3936.65(15)	1315.41(15)	1822.57(4)
Z	4	2	2
cryst color	colorless	red	maroon
ρ(calcd), g cm^{-3}	1.394	1.661	1.569
μ(Mo Kα), cm^{-1}	4.62	6.68	5.03
temp, °C	25	−100	−100
$R(F)$,[a] $R(wF^2)$[a]	0.0644, 0.1793	0.0600, 0.2051	0.0552, 0.1988

[a] Quantity minimized = $R(wF^2) = \sum[w(F_o^2 - F_c^2)^2]/\sum[w(F_o^2)^2]^{1/2}$; $R(F) = \sum\Delta/\sum(F_o)$, $\Delta = |F_o - F_c|$.

Solution NMR Spectral Studies. Solution ^{1}H NMR spectra obtained for **1** at 293 K are broad with chemical shifts ranging from +52 to −42 ppm, a range that is indicative of a paramagnetic HS complex. Lowering the temperature leads to large changes in the positions of the resonances. For example, the resonance for the hydrogen atom on the backbone methine carbon moves from −42.3 to −82.7 ppm and the 4-position hydrogen moves from 51.8 to 80.5 ppm as the temperature is lowered from 293 to 185 K. These shifts are expected from the Curie law behavior of a paramagnetic compound. There is no indication of the formation of any of the LS, diamagnetic complex, as there is in the solid phase at the lower temperatures (vide infra). The formation of a small amount of the diamagnetic complex cannot be ruled out, but it would have to be in fast equilibrium, on the NMR time scale, with the paramagnetic form. Substantial amounts of the diamagnetic form of **1** cannot be present at low temperatures because the temperature dependence of the NMR signals yields larger chemical shifts as the temperature is lowered. If large amounts of the diamagnetic form were present as the temperature is lowered, the spectra should shift toward the lower values expected for a diamagnetic complex, as observed recently, for example, for [Fe(1,4,7-trimethyl-1,4,7-triazacyclonane)$(MeCN)_3$]$(BPh_4)_2$.[15]

In contrast, NMR spectra of **2**, obtained in DMF, are temperature dependent, Figure 1. As shown in Figure 1a, at 223 K a normal spectrum for a diamagnetic form of **2** in the 6−11 ppm range is observed. In addition, at this temperature small resonances shifted from +74.8 to −60.9 ppm are observed and can be attributed to a small amount of **2** present in the HS configuration. These resonances are shown in Figure 1b in which the vertical scale has been increased so as to show the paramagnetic portion of the spectra at the expense of driving the diamagnetic resonances off scale. The highly shielded resonance is assigned to the methine hydrogen on the basis of its relative integration. It should be noted that in complex **1** this resonance is also highly shielded. As the temperature increases, Figure 1b, the relative intensities of the paramagnetic resonances increase such that they represent 22% of the signal at 293 K. In addition, the paramagnetic resonances move to lower absolute chemical shift values. These shifts are expected

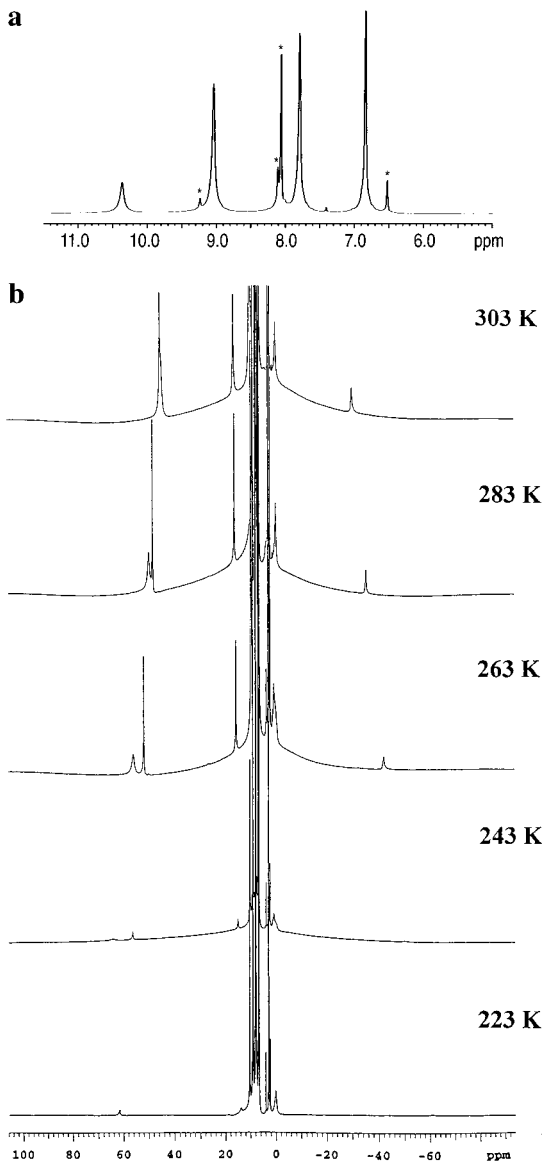

Figure 1. (a, top) Proton NMR (223 K) spectrum of **2** in the region from 6 to 11 ppm (asterisks indicate solvent impurities). (b, bottom) Variable-temperature proton NMR spectra from −80 to +100 ppm of **2**. In the spectra in (b), the vertical scale has been increased, driving the diamagnetic resonances off scale.

for Curie law behavior. Although the resonances for the paramagnetic form are somewhat broad at low temperatures, as expected, they broaden considerably at 303 K, and by 353 K all resonances have collapsed into the baseline. Complex **2** is not stable in DMF above this temperature, but subsequent cooling of the sample reproduced the spectra recorded as the sample was heated, indicating that the process is reversible. As the temperature is increased, the resonances in the diamagnetic form move toward their associated resonances in the paramagnetic form; the methine hydrogen moves to higher shielding, and the other resonances move to lower shielding. Thus, two changes take place as the sample is warmed. First, as expected, the percentage of the paramagnetic form increases as the temperature increases. Second, although the two forms equilibrate slowly on the NMR time scale at 223 K, they start to equilibrate at a rate comparable to the NMR time scale above 283 K.

Observation by NMR of both the HS and LS forms in solutions of **2** is unusual. For example, both Fe$[HB(pz)_3]_2$[3a] and [Fe(1,4,7-trimethyl-1,4,7-triazacyclonane)$(MeCN)_3$]$(BPh_4)_2$[15] show

(15) Blakesley, D. W.; Payne, S. C.; Hagen, K. S. *Inorg. Chem.* **2000**, *39*, 1979.

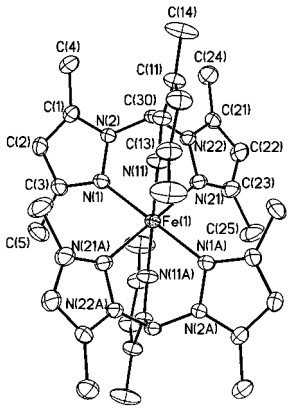

Figure 2. ORTEP diagram of the cation in **1**.

Table 2. Selected Bond Distances and Angles for **1**−**3**

	1	**2**	**3**
Bond Distances (Å)			
Fe−N(1,1(A))	2.155(3)	1.966(3)	1.941(2)
Fe−N(11,11(A))	2.179(2)	1.977(3)	1.970(2)
Fe−N(21,21(A))	2.177(2)	1.972(7)	1.9603(19)
C(30,31)−N(2)	1.444(4)	1.417(5)	1.487(3)
C(30,31)−N(12)	1.451(3)	1.460(4)	1.484(3)
C(30,31)−N(22),C(21)	1.448(4)	1.450(5)	1.543(3)
intraligand donor N···N av distance	2.91	2.72	2.70
distance Fe out of N_3 donor plane	1.373(2)	1.188(2)	1.179(1)
Bond Angles (deg)			
N(1)−Fe−N(11)	84.41(11)	87.74(13)	88.67(8)
N(1)−Fe−N(21)	83.70(10)	86.83(13)	86.74(8)
N(11)−Fe−N(21)	84.67(10)	87.78(12)	86.77(8)
N(1)−Fe−N(11A)	95.59(11)	92.26(13)	91.33(8)
N(1)−Fe−N(21A)	96.30(10)	93.17(13)	93.26(8)
N(11)−Fe−N(21A)	95.33(10)	92.22(12)	93.23(8)
N(1)−N(2)−C(30,31)	119.2(2)	118.7(3)	117.33(18)
N(11)−N(12)−C(30,31)	119.6(2)	117.9(3)	116.27(18)
N(21)−N(22),C(31)−C(30,31)	119.8(2)	118.0(3)	117.57(19)
N(2)−C(30,31)−N(12)	111.4(2)	110.0(3)	105.03(18)
N(2)−C(30,31)−N(22),C(21)	111.9(2)	110.3(3)	110.09(18)
N(12)−C(30,31)−N(22),C(21)	111.1(3)	108.8(3)	108.94(18)
Fe−N(1)−N(2)−C(1) torsion	166.1(2)	177.8(3)	170.4(2)
Fe−N(11)−N(12)−C(11) torsion	168.5(2)	179.6(3)	156.7(2)
Fe−N(21)−N(22),C(21)−C(21,22) torsion	171.4(2)	177.7(3)	170.2(2)

only averaged spectra down to 243 K. Given that the two forms differ in Fe−N bond distances by ca. 0.2 Å,[1] slow exchange might have been expected, as is observed with **2** and a very recently reported tetrameric iron(II) compound.[4f]

The equilibrium constant, K = [HS]/[LS], was determined between 223 and 293 K. The thermodynamic parameters, derived from a plot of ln K vs $1/T$, are $\Delta H° = 20$ kJ/mol and $\Delta S° = 58$ J/(K mol). Similar parameters of $\Delta H° = 18$ kJ/mol and $\Delta S° = 53$ J/(K mol) have been obtained previously for {Fe[HC(pz)$_3$]$_2$}(ClO$_4$)$_2$ from visual absorption spectral data.[9a]

Crystallographic Studies. The solid-state structures of all three complexes have been determined crystallographically at ambient temperature. Figure 2 shows an ORTEP diagram of the cation in **1**.[11] Table 2 gives selected bonds distances and angles. The average Fe−N bond distance is 2.17 Å, clearly indicating that the iron(II) is in a HS configuration at 298 K; average distances of ca. 1.97 Å are typically observed in LS octahedral FeN$_6$ complexes.[1] The iron(II) is located on a unique crystallographic site which lies on a center of symmetry, with an N$_6$ coordination arrangement. The chelate rings restrict the intraligand N−Fe−N angles to averages of 84.3°, corresponding to a trigonally distorted octahedral structure.

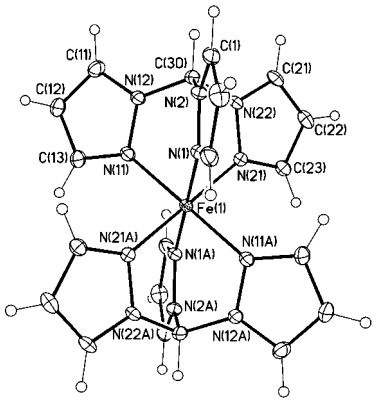

Figure 3. ORTEP diagram of the cation in **2**.

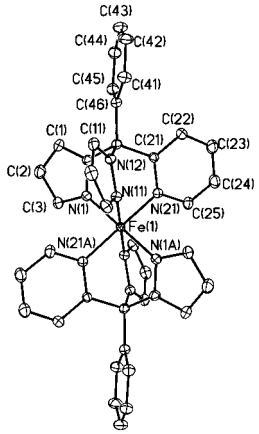

Figure 4. ORTEP diagram of the cation in **3**.

The structure of the cation in **1** is very similar to the structure of Fe[HB(3,5-Me$_2$pz)$_3$]$_2$.[6] The average Fe−N distance in this tris(pyrazolyl)borate complex is identical at 2.17 Å, but the average N−Fe−N angles are greater at 86.6°. As we have discussed previously,[8] the smaller angle observed in the tris(pyrazolyl)methane complex is caused by the expected shorter C(methine)−N bond distance (average 1.45 Å) in the backbone of the ligand compared to the analogous B−N distance (average 1.54 Å) in the tris(pyrazolyl)borate ligand. This change in the backbone of the tris(pyrazolyl)methane ligand decreases its bite angle.

Clear, colorless crystals of **1** can be repeatedly cooled below 200 K (where they turn purple) and reheated to ambient temperature (they go colorless again) without change. Crystals which have been cooled to 120 K remain suitable for X-ray structural studies at ambient temperature.[16]

Figure 3 shows an ORTEP diagram of the cation in **2**, and Table 2 gives selected bond distances and angles. After completion of our work, the structures of two forms of {Fe[HC(pz)$_3$]$_2$}(NO$_3$)$_2$ were reported.[10] The dimensions of the cation in all three structures are similar. The average Fe−N bond distance in **2** is 1.97 Å, essentially the same value as found in both forms of {Fe[HC(pz)$_3$]$_2$}(NO$_3$)$_2$. These distances are important as they clearly indicate that the iron(II) in **2** is in the LS state at 298 K.

Figure 4 shows an ORTEP diagram of the cation in **3**, and Table 2 gives selected bond distances and angles. This structure is the first crystallographic characterization of a complex

(16) X-ray crystallographic results on crystals cooled below 200 K will be reported elsewhere: Reger, D. L.; Little, C. A.; Young, V.; Pink, M. *Inorg. Chem.*, submitted for publication.

containing this new ligand. The asymmetric unit contains two cationic iron(II) complexes and half a molecule of acetone. In one of the cations the pyridyl ring is disordered with one of the pyrazolyl rings; Figure 4 and Table 2 show data for the nondisordered cation.

Despite the asymmetry of this tripodal ligand, in having both different types of donor rings and the phenyl group on the central carbon atom, the FeN_6 central core is rather regular with an average Fe−N distance of 1.96 Å, a distance that is very close to that observed in **2**. Clearly complex **3** is LS at room temperature. The structure of {Fe[HC(pz)$_2$py]$_2$}(NO$_3$)$_2$ has been reported[17] and has the same average Fe−N distance as observed in **3**. In this structure the largest difference in Fe−N bond lengths is only 0.006 Å, whereas in **3** it is 0.029 Å. In tris(pyrazolyl)-borate chemistry, substitution of the hydrogen atom bonded to boron in the parent $[HB(pz)_3]^-$ ligand with a pyrazolyl or phenyl ring frequently leads to the introduction of considerable asymmetry in the iron(II) coordination environment or sometimes even to a change in the coordination of the ligand to bidentate because of the unfavorable interactions among the rings.[18] For example, in Fe[HB(pz)$_3$]$_2$ the Fe−N bond distances vary by only 0.008 Å,[6] whereas in Fe[PhB(pz)$_3$]$_2$ they vary by 0.211 Å.[18a] It is not clear why greater asymmetry is not observed in **3**. Given the shorter central carbon C(31) to ring distances as compared with the analogous boron B-ring distances, greater asymmetry might have been expected.

Comparison of the structures of the cations in LS **2** with those in HS **1** indicates why the iron(II) favors the different spin states. Sohrin has reported such an analysis on the tris(pyrazolyl)borate analogues.[18a] Following this analysis, interligand steric repulsions between the 3-position methyl groups in {Fe[HC(3,5-Me$_2$-pz)$_3$]$_2$}$^{2+}$ favor the HS state that has the 0.2 Å longer Fe−N bond distances. Even in the HS state {Fe[HC(3,5-Me$_2$pz)$_3$]$_2$}-(BF$_4$)$_2$ has C···C nonbonding distances between adjacent interligand 3-methyl groups that average 3.75 Å, a value which is less than the 4.0 Å sum of the van der Waals radii of two methyl groups.[19]

The tris(pyrazolyl)methane ligands change their configurations in a number of ways to accommodate the larger HS iron(II). As is shown in Table 2, the HC(3,5-Me$_2$pz)$_3$ ligand opens its "bite size" by expanding the intraligand donor N···N distance by 0.19 Å as compared with that in HC(pz)$_3$ in complex **2**. This opening is realized by increasing the backbone N−C(30)−N and N−N−C(30) angles. In addition, the degree of tilting the pyrazolyl rings make away from an ideal C_{3v}-type arrangement increases in **1**. In the absence of tilting, the FeN(n1)−N(n2)−C(n1) angles, where n denotes the ring number, would be 180° and the metal atom would reside in the planes defined by the pyrazolyl rings. In complex **2** this angle averages 178.4°, whereas in **1** it is 168.7°. With very large metals, such as thallium(I), this tilting can be 123°.[8g] Even with these ligand structural adjustments, the iron(II) in **1** sits nearly 0.2 Å farther from the N_3 intraligand planes than in **2** and **3** because of the longer Fe−N bond distances. These subtle changes of the bonding properties permit the tris(pyrazolyl)-methane and tris(pyrazolyl)borate ligands to form stable complexes with metals of very different ionic radii. Nevertheless, interactions of the 3-position methyl groups in **1** favor the HS state with the longer Fe−N distances.

(17) Astley, T.; Canty, A. J.; Hitchman, M. A.; Rowbottom, G. L.; Skelton, B. W.; White, A. H. *J. Chem. Soc., Dalton Trans.* **1991**, 1981.
(18) (a) Sohrin, Y.; Kokusen, H.; Matsui, M. *Inorg. Chem.* **1995**, *34*, 3928. (b) Reger, D. L.; Huff, M. F.; Rheingold, A. L.; Haggerty, B. S. *J. Am. Chem. Soc.* **1992**, *114*, 579. (c) Reger, D. L. *Synlett* **1992**, 469.
(19) Bondi, A. *Phys. Chem.* **1964**, *68*, 441.

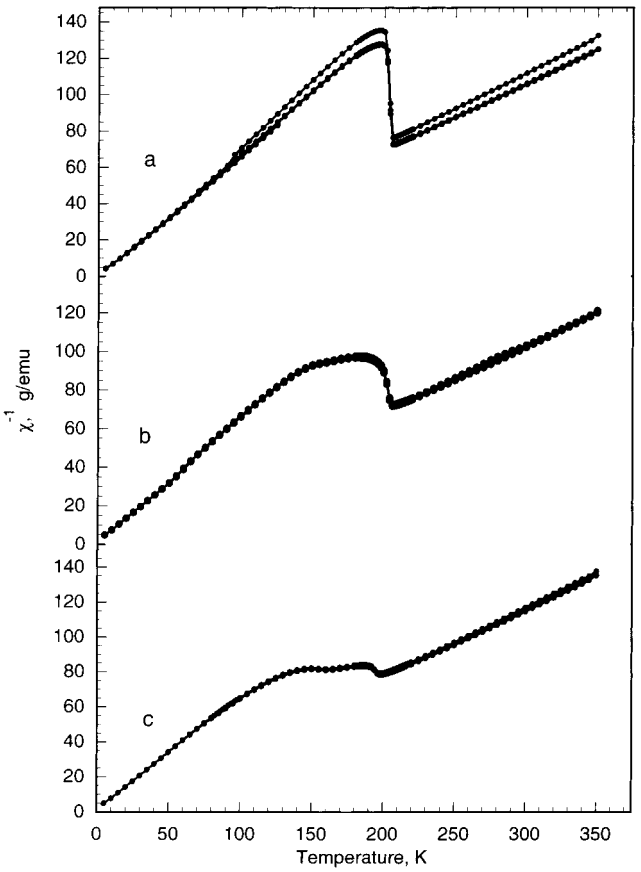

Figure 5. Inverse magnetic susceptibility as a function of temperature of **1** obtained on unground crystallites (a), thoroughly ground crystallites (b), and powder (c). The data in (a) were collected by cooling a crystalline sample from 350 to 5 K, followed by heating back to 350 K and recooling to 5 K. The curve with greater inverse magnetic susceptibility (top curve) from 350 to 90 K corresponds to the initial cooling. After the slight change at 90 K, all subsequent data from cooling, heating, and recooling superimpose. Plots b and c show superimposed measurements taken as the samples were initially cooled from 350 to 5 K, then heated to 350 K, and finally cooled again to 5 K.

Magnetic Studies. {Fe[HC(3,5-Me$_2$pz)$_3$]$_2$}(BF$_4$)$_2$ (1). Figure 5a shows the inverse magnetic susceptibility versus temperature of **1**, obtained on a crystalline sample. These results indicate that upon initial cooling **1** is HS from 350 to 206 K and exhibits Curie law behavior with a μ_{eff} of 4.77 μ_B (top curve in Figure 5a). Below 206 K complex **1** undergoes a very abrupt increase in the inverse susceptibility. Then after the abrupt change, the inverse susceptibility again shows Curie law behavior between ca. 190 and 90 K with a μ_{eff} of 3.49 μ_B, a magnetic moment that corresponds to a ca. 50:50 mixture of HS and LS iron(II) in an octahedral environment. At 90 K the inverse susceptibility shows a slight, but clearly reproducible, decrease. From 85 to 5 K the inverse susceptibility again follows the Curie law with a μ_{eff} of 3.55 μ_B.

Upon warming, the inverse susceptibility of **1** follows the 85 to 5 K cooling line *all the way up to 200 K*; i.e., it does not show the slight change in inverse susceptibility at 90 K that was observed on cooling. Then a very abrupt decrease in the inverse susceptibility is observed at ca. 200 K, a change which is similar to that observed during the initial cooling. After this abrupt decrease the inverse susceptibility does *not* follow the initial cooling line but does exhibit Curie law behavior with a μ_{eff} of 4.88 μ_B, a moment which corresponds to an increase in μ_{eff} of 0.11 μ_B compared to that of the first cooling line. During the second cooling from 350 to 5 K, the inverse susceptibility

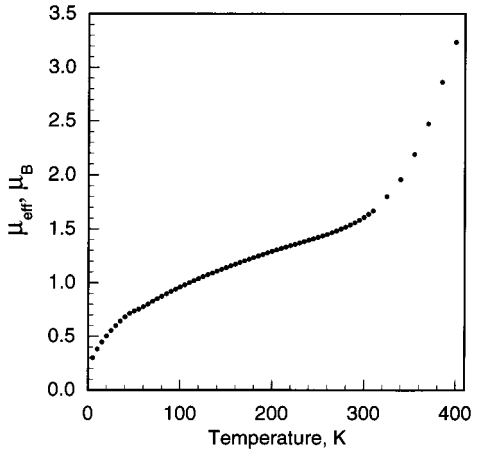

Figure 6. Effective magnetic moment (μ_B) of **2** as a function of temperature (K).

is superimposed upon *the initial warming plot* and shows only one abrupt increase starting at 206 K. Again the magnetic moments correspond to the sample being fully HS at high temperature, changing over to a 50:50 mixture at low temperatures of HS and LS iron(II). There is no observable hysteresis in these cooling and heating plots except that the initial small decrease in the inverse susceptibility at 90 K is an irreversible change that permanently increases the magnetic moment of the paramagnetic form at all temperatures. Similar magnetic behavior is observed at fields ranging from 5 to 40 kG. When fresh crystals are cooled from 350 to 220 K and then reheated to 350 K, the warming plot follows exactly the initial cooling plot shown in Figure 5a. These crystals were then cooled below 90 K and behaved exactly the same as shown in Figure 5a, showing the one-time irreversible change at ca. 90 K.

Figure 5b shows the inverse magnetic susceptibility of complex **1** measured on the *same* crystalline sample that was used for the measurements described above and shown in Figure 5a *except* that in this case the sample had been finely and thoroughly ground in a mortar and pestle after the earlier magnetic studies. It is apparent that grinding has a major impact on the abruptness of the spin-state crossover. Importantly, the high- and low-temperature magnetic moments are the *same* as with the crystalline sample. Thus, grinding crystalline complex **1** alters the abruptness of the spin-state change, but once the change is complete, the same magnetic moments are obtained at both high and low temperatures with and without grinding.

Figure 5c shows the inverse magnetic susceptibility of **1** measured on the powder that forms in the original reaction. In this case the spin-state crossover is again observed, but is much less abrupt than even for the ground sample. Also, only a very small change is observed the first time the sample is cooled below 90 K. It is likely that the small abrupt change at 200 K and the very small change at 90 K result from a small amount of microcrystalline material in the powder. As observed with the ground sample, even though the spin-state change is much more gradual than with the crystalline sample, the high- and low-temperature moments again match those of the crystalline sample. Grinding the crystalline sample or using a powder sample changes the cooperative effects in the solid that must be operating to produce the abrupt change in the crystalline sample, but does not influence the final composition of the spin-state crossover.

{Fe[HC(pz)$_3$]$_2$}(BF$_4$)$_2$ (2). Figure 6 shows the magnetic moment of **2** as a function of temperature. The magnetic moment of this complex is 0.3 μ_B at 5 K and 0.74 μ_B at 50 K, results that are analogous to those reported by others for the same cation with ClO_4^- [9a] or NO_3^- [10] as the counterion. These values arise from a predominately diamagnetic $^1A_{1g}$ state plus a contribution of a second-order Zeeman-derived temperature-independent susceptibility.[10] There is no indication in the Mössbauer spectra of **2** (vide infra) of the presence of any measurable amount of an iron(III) species. As the temperature is increased above 50 K, the magnetic moment rises slowly to ca. 320 K, where it starts to increase rapidly, rising to 3.24 μ_B at 400 K. Although the magnetic moment could not be measured quantitatively above 400 K, data collected from 300 to 600 K using a high-temperature probe show that the moment of **2** continues its gradual increase above 400 K, with the changeover essentially complete above 470 K. This change is reversible; the cooling curve closely follows the warming curve. The change can also be observed visually as the purple sample turns completely white by 600 K when heated in a sealed capillary tube during a melting point determination, changing back to purple as it is cooled.

Table 3. Selected Mössbauer Spectral Parameters

complex	T, K	δ,[a] mm/s	ΔE_Q, mm/s	Γ, mm/s	rel area, %	assignment
1	295[b]	0.966	3.96	0.27	50	high-spin, A
		1.043	3.78	0.27	50	high-spin, B
	280[c]	0.989	3.97	0.29	50.0	high-spin, A
		1.064	3.80	0.29	50.0	high-spin, B
	210[b]	0.505	0.21	0.24	53.4	low-spin
		1.023	3.99	0.29	23.3	high-spin, A
		1.116	3.80	0.29	23.3	high-spin, B
	210[c]	0.510	0.23	0.29	58.4	low-spin
		1.021	3.99	0.29	20.8	high-spin, A
		1.114	3.81	0.29	20.8	high-spin, B
	209[c]	0.510	0.23	0.28	30.0	low-spin
		1.027	3.98	0.29	35.0	high-spin, A
		1.117	3.80	0.29	35.0	high-spin, B
	205[b]	0.505	0.20	0.25	44.0	low-spin
		1.027	3.99	0.29	28.0	high-spin, A
		1.114	3.80	0.29	28.0	high-spin, B
	85[b]	0.529	0.20	0.26	51.6	low-spin
		1.107	3.99	0.26	24.2	high-spin, A
		1.155	3.77	0.26	24.2	high-spin, B
	60[d]	0.530	0.20	0.29	51.8	low-spin
		1.104	3.93	0.27	24.1	high-spin, A
		1.165	3.79	0.27	24.1	high-spin, B
	20[d]	0.532	0.20	0.27	50.8	low-spin
		1.130	3.91	0.25	24.6	high-spin, A
		1.145	3.81	0.25	24.6	high-spin, B
	4.2	0.532	0.19	0.23	48.4	low-spin
		1.136	3.90	0.24	25.8	high-spin, A
		1.139	3.81	0.24	25.8	high-spin, B
2	472	0.744	2.98	0.35	100	high-spin
	295	0.416	0.22	0.30	100	low-spin
	78	0.475	0.23	0.29	100	low-spin
	4.2	0.448	0.25	0.25	100	low-spin
3	295	0.339	0.42	0.25	100	low-spin
	78	0.404	0.41	0.29	100	low-spin

[a] The isomer shifts are given relative to room-temperature α-iron foil. [b] Data obtained during the initial cooling to 85 K. [c] Data obtained during warming after the initial cooling to 85 K. [d] Data obtained during warming from 4.2 K.

Mössbauer Spectral Analysis. The variable-temperature Mössbauer spectra of **1** are shown in Figure 7, and selected hyperfine parameters for this complex are given in Table 3. Spectra were measured as the sample was cooled from 295 to 85 K and then heated from 85 to 295 K. The sample was then cooled to 4.2 K, and spectra were measure as it was warmed from 4.2 to 220 K. The complete temperature dependencies of the isomer shift for the HS and LS states and the quadrupole splitting for the HS iron(II) states are shown in Figures 8 and 9. As the sample is cooled, there is a dramatic change in the

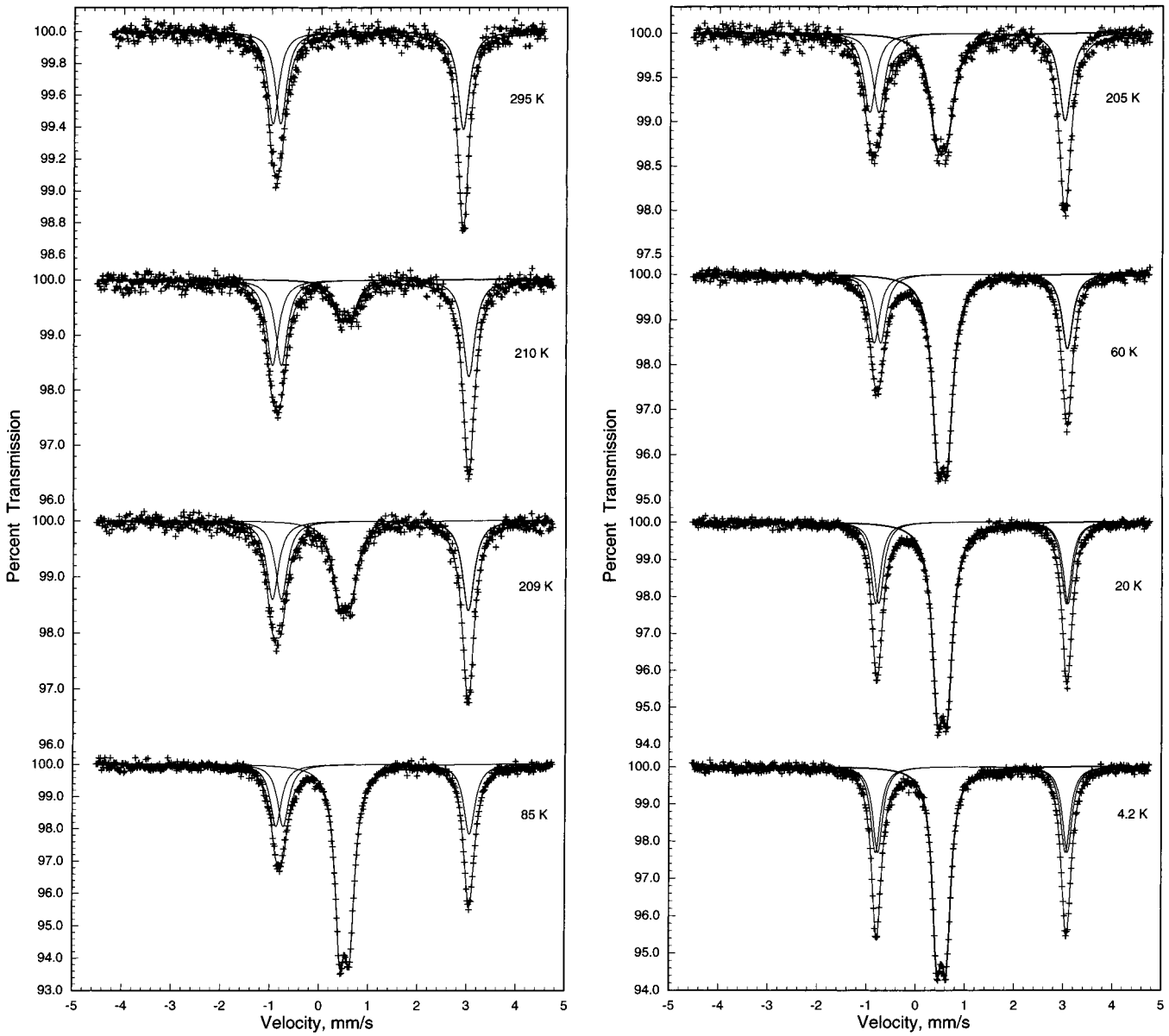

Figure 7. Mössbauer spectra of **1** obtained at the indicated temperatures upon warming from 85 K (a, left) and from 4.2 K (b, right).

spectra starting at 210 K that indicates that the sample is changing from completely HS to a mixture of HS and LS.[1] The change in population of the HS state, as reflected by the Mössbauer spectral absorption area of the HS spectral components, is shown in the inset of Figure 8.

The hyperfine parameters reported in Table 3 are those expected for HS and LS iron(II) complexes with a distorted pseudooctahedral coordination geometry. The HS and LS isomer shifts at 78 K for **1** are virtually identical to those of the analogous tris(pyrazolyl)borate complex Fe[HB(3,5-Me_2pz)$_3$]$_2$. However, the 295 K quadrupole splittings of 3.78 and 3.96 mm/s observed for **1** are significantly higher than the 3.65 mm/s value observed for Fe[HB(3,5-Me_2pz)$_3$]$_2$, indicating a more distorted iron(II) coordination environment in **1**, a distortion which is consistent with the larger angular distortion observed in its X-ray structure; see discussion above. Although the spectra of Fe[HB(3,5-Me_2pz)$_3$]$_2$ can always be fit with one HS doublet, complex **1** requires two HS doublets at all temperatures above ca. 30 K, a requirement that has been confirmed for spectra obtained with two separate preparations of **1** on two different Mössbauer spectrometers.

There are two aspects of the Mössbauer spectral results shown in Table 3 and Figures 7−9 that are unexpected and require special comment. The first is the necessity, as shown in Figure 7, of using two doublets to fit the HS iron(II) spectra of **1**. Any attempt to fit the HS absorption measured at temperatures above 30 K with a single doublet results in very poor fits. The second is the failure of all of the HS iron(II) in **1** to be converted to the LS state upon cooling. As is shown in the inset of Figure 8, and in agreement with the magnetic results discussed above, only ca. 50% of the HS iron(II) is converted to the LS state. It might have been expected that one of the HS iron(II) doublets would have disappeared upon conversion to the LS state, but this clearly is *not* the case as is shown at 205 K and below in Figure 7b.

The observation of two HS iron(II) doublets in **1** is unexpected in view of the unique crystallographic iron(II) site revealed by the single-crystal X-ray diffraction results reported herein. However, in an earlier study[20] of the Mössbauer spectra of Fe[B(3-isopropylpyrazol-1-yl)$_4$]$_2$, which contains iron(II) in

(20) Long, G. J.; Grandjean, F.; Trofimenko, S. *Inorg. Chem.* **1993**, *32*, 1055.

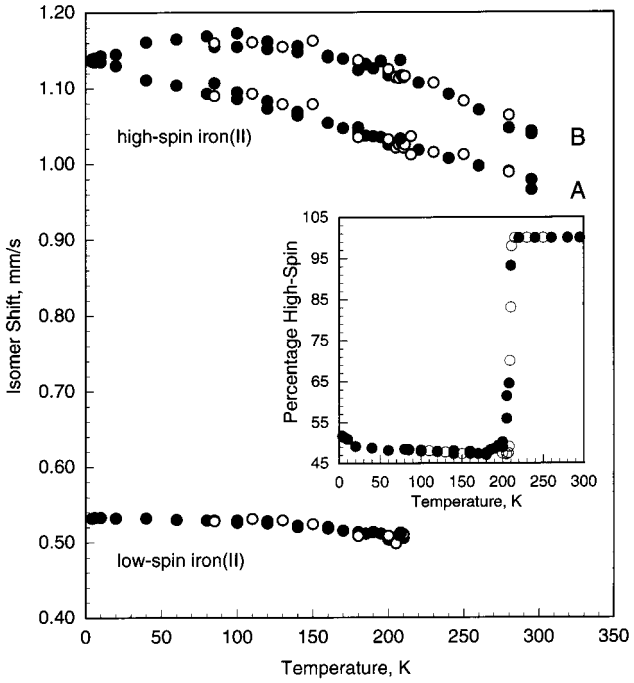

Figure 8. Temperature dependence of the Mössbauer spectral isomer shifts for **1**. Inset: Temperature dependence of the percentage of high-spin iron(II) found in **1**. The data obtained upon initial cooling from 295 to 85 K and warming from 4.2 K are indicated by ●, and the data obtained upon initial warming from 85 to 280 K are indicated by ○.

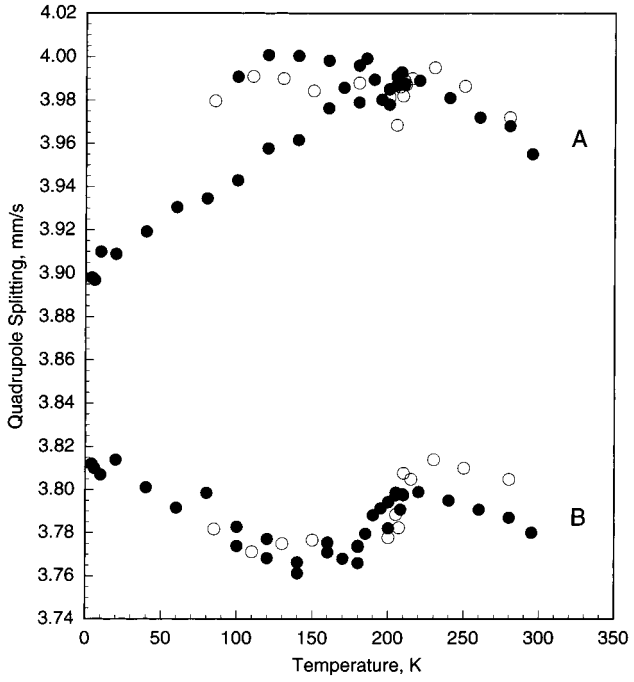

Figure 9. Temperature dependence of the Mössbauer spectral quadrupole splittings for the high-spin iron(II) in **1**. The data obtained upon initial cooling from 295 to 85 K and warming from 4.2 K are indicated by ●, and the data obtained upon initial warming from 85 to 280 K are indicated by ○.

a pseudotetrahedral coordination environment, a similar requirement of two doublets was also observed, even though single-crystal X-ray structural work[21] indicated the presence of only one crystallographically distinct iron(II) site. The two doublets are observed at all temperatures between 85 and 295 K in both **1** and Fe[B(3-isopropylpyrazol-1-yl)$_4$]$_2$. It should be noted that the 295 K quadrupole splittings of 3.78 and 3.96 mm/s for **1** and 4.12 and 4.30 mm/s for Fe[B(3-isopropylpyrazol-1-yl)$_4$]$_2$ are very large. It appears that, sometimes when the quadrupole splitting is this large, its high sensitivity[22] to the local electronic environment of the iron(II) ion may reveal subtle differences in the electronic and structural environment, differences that are not apparent in the X-ray structural refinement.

It should be noted that the hyperfine parameters of the two HS iron(II) quadrupole doublets in {Fe[HC(3,5-Me$_2$pz)$_3$]$_2$}-(BF$_4$)$_2$, referred to herein as A and B, vary somewhat differently with temperature and, indeed, approach each other at temperatures below ca. 30 K; see Figures 7b, 8, and 9. Further, it appears that the observed spectra depend somewhat upon the thermal history of the sample. The quadrupole splittings obtained on warming from 4.2 K, after the sample was cooled below 85 K for the first time, are somewhat different from those obtained upon warming from 85 K. Although the differences are small, they are real and reproducible. These changes match the change in magnetic properties where an irreversible change is observed between 85 and 90 K; see Figure 5a. Thus, both the Mössbauer spectral and magnetic studies indicate that there is a small, irreversible change in the sample when it is cooled below 85 K.

In contrast to the quadrupole splittings, as shown in Figure 8 there are no differences in the isomer shifts upon warming from 4.2 or 85 K. Upon both cooling and warming, the isomer shift of doublet A shows a nearly linear change with temperature whereas the isomer shift of doublet B shows some curvature with a maximum at ca. 100 K. Concurrently, as shown in Figure 9, the quadrupole splitting of doublet A increases upon warming from 4.2 to 200 K and then decreases, whereas the splitting of doublet B shows a distinct decrease upon warming from 4.2 to 200 K and then increases slightly at the spin crossover.

The spin-state crossover in **1** is superficially similar to that observed[23] for [Fe(1-methyl-1*H*-tetrazole)$_6$](BF$_4$)$_2$, in which only 50% of the iron(II) is converted to the LS state upon cooling. However, in this complex there are two crystallographically different iron(II) sites, and in Mössbauer spectral studies the disappearance of only one of the HS iron(II) doublets was observed, indicating that one site changes completely from HS to LS and the other remains HS. For **1**, crystallographically there is only one iron(II) site, and the two iron(II) sites observed by Mössbauer spectroscopy are present both above and below the spin-crossover temperature, so that it is *not* possible to conclude that only one of the two doublets is transformed from the HS to the LS state upon cooling.

Quite recently, van Koningsbruggen et al.[24] have reported a spin-state crossover in {Fe[μ-tris(1,2-bis(tetrazol-1-yl)propane-*N*1,*N*1′]}(ClO$_4$)$_2$ and found two unexpected quadrupole doublets with splittings of 1.11 and 1.30 mm/s at 300 K for the HS state even though there is only one iron(II) site with a nearly perfect octahedral environment. They proposed that the presence of the two doublets above and below the spin-crossover temperature results from disorder of the methyl groups on the propane bridge in this complex. A similar explanation in the case of complex **1** is clearly not indicated in the above X-ray structural work; there is no structural disorder observed in **1**.

(21) Rheingold, A. Unpublished results.

(22) Reiff, W. M.; Long, G. J. In *Mössbauer Spectroscopy Applied to Inorganic Chemistry*; Long, G. J., Ed.; Plenum: New York, 1984; Vol. 1, p 245.

(23) Poganiuch, P.; Decurtins, S.; Gütlich, P. *J. Am. Chem. Soc.* **1990**, *112*, 3270.

(24) van Koningsbruggen, P. J.; Garcia, Y.; Kahn, O.; Fournès, L.; Kooijman, H.; Spek, A. L.; Haasnoot, J. G.; Moscovici, J.; Provost, K.; Michalowicz, A.; Renz, F.; Gütlich, P. *Inorg. Chem.* **2000**, *39*, 1891.

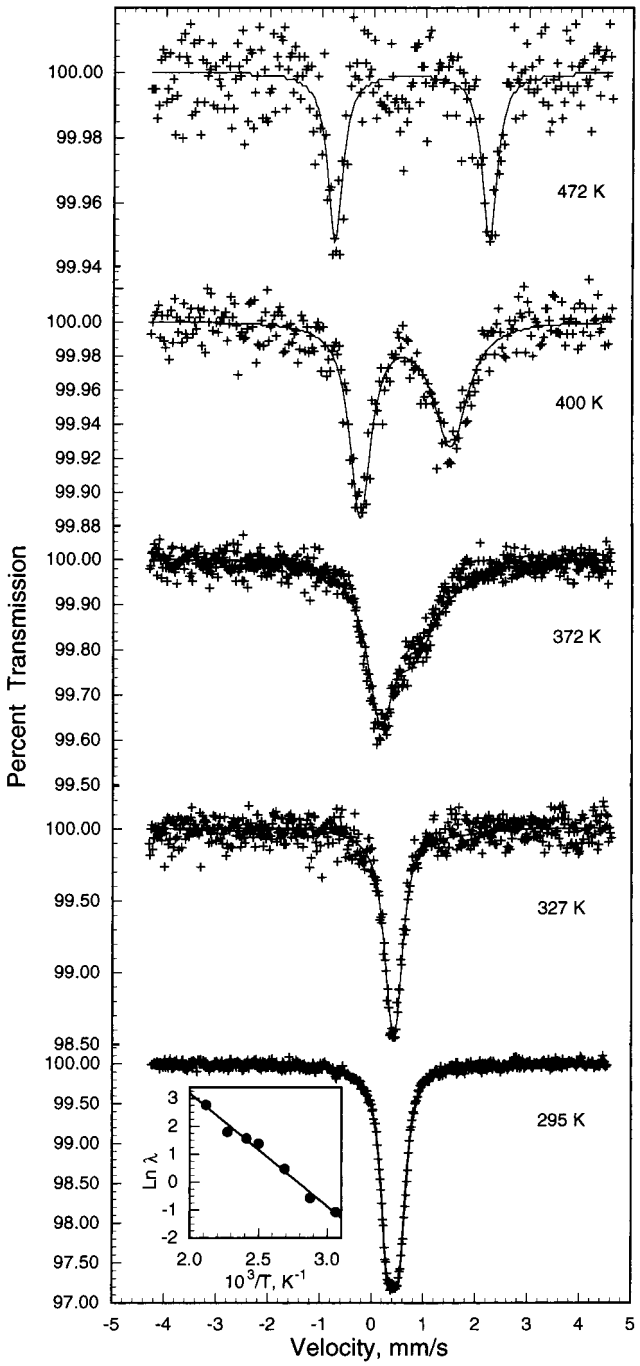

Figure 10. Mössbauer spectra of **2** obtained at the indicated temperatures and fit with a model for relaxation between the high-spin and low-spin electronic states. Inset: An Arrhenius plot of the high-spin low-spin relaxation rate in **2**. The slope corresponds to an activation energy of 2820 cm^{-1}. The error bars for the relaxation rates are approximately twice the size of the data points.

As shown in Figure 10, **2** is fully LS at 295 K. The isomer shift and the quadrupole splitting are essentially identical to those of Fe[HB(pz)$_3$]$_2$.[2] In view of the increase in the magnetic moment of **2** above 295 K, see Figure 6, the Mössbauer spectra of **2** have been measured between 295 and 472 K, and some of the results are shown in Figure 10. It is difficult to obtain high-temperature spectra of this complex because its recoil-free fraction decreases dramatically upon heating, especially above 400 K. Indeed, over 66 million counts per channel or over 17 $\times$ 10^9 γ-rays were counted over the 9 days required to obtain the 472 K spectrum shown in Figure 10. Significantly, however, the 295 K spectrum of **2** obtained after the 472 K spectrum is identical to that observed before heating, indicating that no iron(II) oxidation has occurred. The spectra shown in Figure 10 clearly reveal that upon heating above ca. 295 K complex **2** begins to undergo spin-state relaxation between its LS and HS states on the Mössbauer time scale. This relaxation is clearly indicated at 400 K by the presence of the broad absorption at ca. 1.5 mm/s, an absorption which shifts to higher energy and sharpens at higher temperatures. At 472 K the spectrum is a symmetric doublet with hyperfine parameters, see Table 3, that indicate that **2** is essentially completely HS at this temperature. It is also significant that the spectrum obtained at 327 K is narrower than the spectrum observed at 295 K. This is a clear indication that the signs of the quadrupole splittings of the HS and LS states in **2** must be different.

The spectral fits between 327 and 440 K, see Figure 10, have been obtained with the Litterst and Amthauer model for relaxation[25] between two quadrupole doublets[2] with a fixed line width of 0.325 mm/s, the average of the line widths observed at 295 and 472 K; see Table 3. Further, the 295 and 472 K hyperfine parameters for **2** listed in Table 3 have been used as the limiting parameters for the two spin states, and the splitting of the HS state has been taken as $-$2.98 mm/s. It was not possible to model the observed spectra with limiting quadrupole splittings of the same sign, although, as expected, the alternative different signs for the two splittings yielded identical fits. A similar change in sign for the quadrupole splittings in {Fe[HC(pz)$_3$]$_2$}(PF$_6$)$_2$ has been noted previously.[9b]

The relaxation fits shown in Figure 10 yield the relaxation rate, λ, between the two spin states in **2**, relaxation rates which exhibit the expected Arrhenius temperature dependence shown in the inset of Figure 10. The slope of this plot yields an activation energy for the relaxation of 2820 cm^{-1}, an energy which is intermediate between the 7300 and 1760 cm^{-1} values observed,[2] respectively, for the initial heating and the subsequent cooling and reheating of Fe[HB(pz)$_3$]$_2$. It should be noted that iron-57-enriched samples were used in the earlier high-temperature study[2] whereas the work reported herein used natural abundance iron. Thus, as a result of the much poorer signal-to-noise ratio of the spectra in Figure 10, as compared to those reported earlier,[2] it was not possible to observe any differences in the spectra of **2** upon heating and cooling. However, it should be noted that the 472 K hyperfine parameters reported for **2** in Table 3 are quite similar to those observed[2] at 430 K for Fe[HB(pz)$_3$]$_2$, the highest temperature at which it could be studied. But it was not necessary to use different signs[2] for the quadrupole splitting of the two spin states in Fe[HB(pz)$_3$]$_2$ to model its relaxation. The reason for this difference is not certain at this point but may be related to the disposition of the BF$_4^-$ anions about the cation in **2**. This disposition may also explain why the 472 K quadrupole splitting of 2.98 mm/s observed for the high spin state of **2** is slightly smaller than the 430 K quadrupole splitting of 3.15 mm/s observed for the high spin state of Fe[HB(pz)$_3$]$_2$.

An earlier study of {Fe[HC(pz)$_3$]$_2$}(PF$_6$)$_2$ between 200 and 400 K has been reported by Winkler et al.,[9b] and as expected, the 200 to 300 K spectra and the resulting isomer shifts are quite similar to those reported herein for **2**. However, at 350 and 400 K the earlier spectra[9b] are quite different from those shown in Figure 10. Indeed, the 400 K spectrum reported earlier[9b] has a very poor signal-to-noise ratio, and the high-velocity component of the quadrupole doublet is just barely

(25) Litterst, F. J.; Amthauer, G. *Phys. Chem. Miner.* **1984**, *10*, 250.

visible. Because the spectra shown in Figure 10 clearly indicate that at 472 K complex **2** is completely high-spin, the analysis of the spectra and the consequent relaxation rates found herein are somewhat different from the analysis and results reported earlier, which found[9b] an activation energy for the spin transition of either 1500 or 2500 cm^{-1} depending upon how the relative populations of the two spin states were extracted from the observed Mössbauer spectra. The latter value agrees rather well with the activation energy of 2820 cm^{-1} obtained herein for complex **2**.

As expected, see Table 3, the Mössbauer spectral hyperfine parameters for **3** are completely consistent with the presence of low-spin iron(II) in this complex. The isomer shift for **3** is substantially smaller than that of complex **2**, a decrease which is consistent with the shorter Fe−N bond distances in **3**, see Table 2, and the consequent increase of the s-electron density at the low-spin iron(II) nucleus. In contrast, the quadrupole splitting of **3** is almost double that of **2**, an increase which is consistent with the increased distortion of the pseudooctahedral coordination environment about the iron(II) in **3** as compared to **2**.

XANES Spectral Analysis. The 295 and 78 K X-ray absorption near-edge structure spectra, the XANES spectra, of **2** and **1** are shown in parts a and b, respectively, of Figure 11. This figure also shows the changes in the absorption which occur upon cooling from 295 to 78 K. The spectra of **2** are very similar to those reported[26,27] for $Fe[HB(pz)_3]_2$, and the conventional labels have been used for the different observed peaks, whose energies and intensities are given in Table 4. The position and shape of the edge jump are identical for both complexes, but the shape of absorption C is broader in $Fe[HB(pz)_3]_2$ than in **2**, and its intensity is higher at 295 K. Further, in **2** an additional absorption line is observed between lines C and D at 78 K. As expected, because **2** is LS at both 295 and 78 K, there is little change in its spectrum upon cooling, and the assignments of the different bands are essentially identical to that discussed[26] for $Fe[HB(pz)_3]_2$. In addition, full multiple scattering calculations,[28] which have been very successful in reproducing the entire XANES line shape profiles of **1** and **2**, have indicated that the additional structure observed at ca. 20 eV in Figure 11a at 78 K arises from multiple scattering events involving the carbon atoms at ca. 4.0 Å, the carbon atoms in **2** which replace the boron atoms in $Fe[HB(pz)_3]_2$.

The 295 K XANES spectrum of **1** is shown in Figure 11b, and although the changes observed upon cooling to 78 K are not dramatic, they are clearly revealed by the difference plot shown in this figure. At 295 K the spectrum is virtually identical to that reported[26] for $Fe[HB(3,5\text{-}Me_2pz)_3]_2$, and the energies and intensities of the peaks are given in Table 4. As expected the XANES spectrum of **1** partially changes toward that expected of a low-spin iron(II) complex upon cooling. This change is best illustrated by noting the differences which occur, see Figure 11c, in linear combinations of the 295 K low-spin iron(II) XANES spectrum of **2** with the 295 K high-spin iron(II) XANES spectrum of **1**. The major differences are an increase in intensity of spectral absorption D and a shift to higher energy of peak C with a decrease in intensity upon increasing the low-spin content. These changes are exactly those observed in the difference plot for **1** shown in Figure 11b, although their magnitude seems to be somewhat smaller than one might expect for a 50% change in spin state.

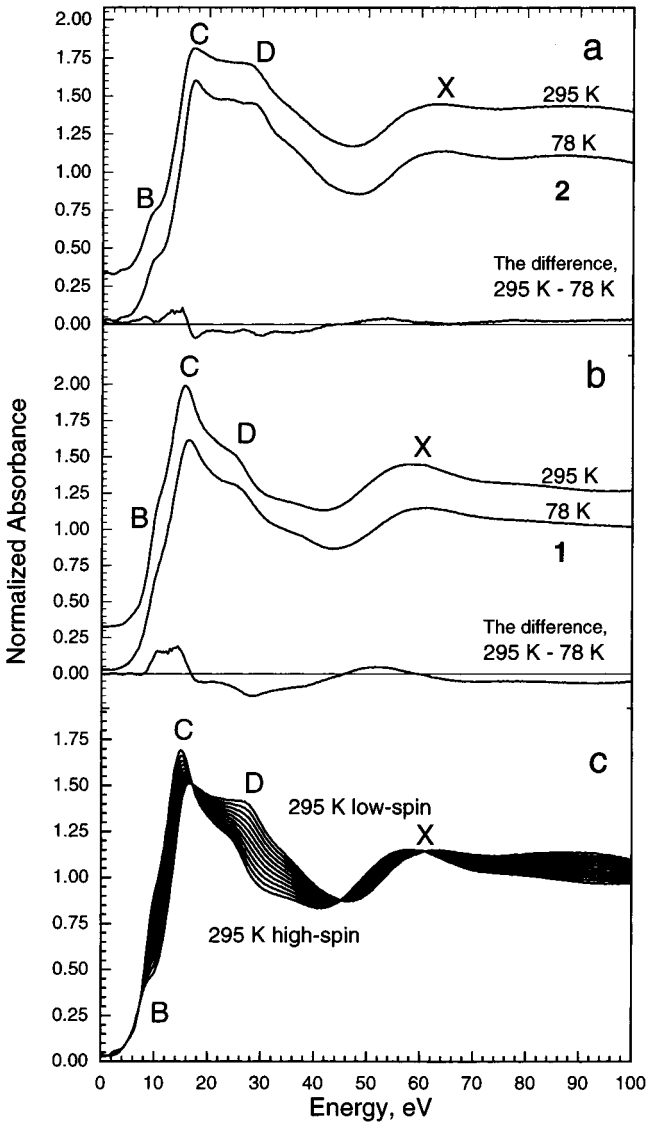

Figure 11. XANES spectra of **2** (a) and **1** (b) measured at 295 and 78 K. The differences between the 295 and 78 K spectra are also shown. A plot of the changes expected in the XANES spectra as iron(II) is converted from the high-spin to the low-spin state (c). In (c) the various spectra were obtained by taking linear combinations of the 295 K XANES spectra of high-spin **1** and low-spin **2**. Thus, the lowest curve at 25 eV corresponds to 100% of a high-spin complex, whereas the highest curve corresponds to a low-spin complex.

Table 4. Relative Energies[a] and Intensities of the XANES Transitions

complex		*T*, K	P	B	C	D	E
1	energy	295	1.6	10.8	15.6	27.5	59.8
	intensity		0.03	0.99	1.63	1.12	1.14
	energy	78	1.4	11.1	16.3	24.7	60.5
	intensity		0.03	0.86	1.58	1.18	1.14
2	energy	295	0.9	10.0	17.1	26.7	62.2
	intensity		0.03	0.48	1.50	1.41	1.15
	energy	78	1.6	10.8	16.2	23.9	61.3
	intensity		0.03	0.45	1.51	1.42	1.16

[a] Absorption energies (eV) relative to the 7112 eV K-edge of iron. The accuracy of the C absorption line is ±0.25 eV, of the P and B lines ±0.5 eV, and of the D and E lines ±0.75 eV.

(26) Hannay, C.; Hubin-Franskin, M. J.; Grandjean, F.; Briois, V.; Itié, J. P.; Polian, A.; Trofimenko, S.; Long, G. J. *Inorg. Chem.* **1997**, *36*, 5580.
(27) Zamponi, S.; Gambini, G.; Conti, P.; Gioia Lobbia, G.; Marassi, R.; Berrettoni, M.; Cecchi, P. *Polyhedron* **1995**, *14*, 1929.
(28) Briois, V.; Sainctavit, Ph.; Long, G. J.; Grandjean, F. *Inorg. Chem.* **2001**, *40*, 912−918.

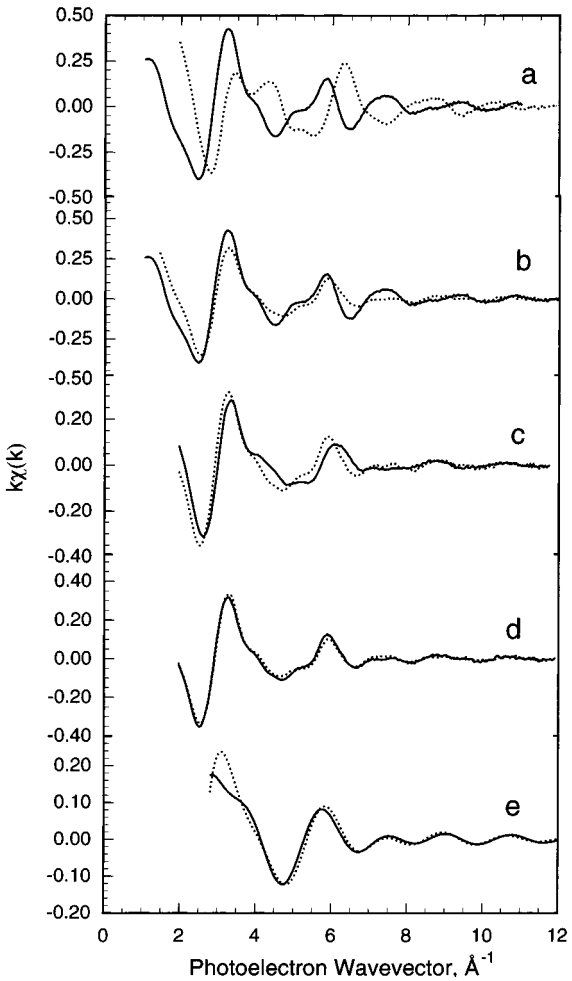

Figure 12. EXAFS (295 K) oscillations observed for high-spin **1** (solid line) and low-spin **2** (dotted line) (a). EXAFS oscillations for **1**, observed at 295 K (solid line), and at 78 K (dotted line) (b). EXAFS (78 K) oscillations obtained for **1** (solid line) and a simulation of the complex oscillations which would result from a 50:50 mixture (c) or a 30:70 mixture (d) of low-spin **2** (solid line) and high-spin **1** (dotted line). EXAFS (78 K) oscillations obtained for **1** (dotted line) and a simulation (solid line) with the parameters given in Table 5 (e).

EXAFS Spectral Analysis. The 295 K EXAFS oscillations extracted from the X-ray scattering measured to ca. 1000 eV above the iron K-edge absorption for **1** and **2** are shown in Figure 12a. These oscillations are quite different because of the differing iron−nitrogen bond lengths in the HS and LS states of **1** and **2**, respectively, at this temperature. The oscillations obtained at 295 and 78 K for **1** are shown in Figure 12b. In this case there are subtle differences in the oscillations because at 78 K **1** is a mixture of HS and LS iron(II) with different bond lengths. The Fourier transforms of the 295 K oscillations shown in Figure 12a are given in Figure 13a. These transforms clearly indicate the longer bond lengths expected in HS **1**, as compared to LS **2**.

The Fourier transforms, shown at 295 K in Figure 13a, as well as those obtained at 78 K have been filtered and then back-Fourier-transformed to obtain only the oscillations resulting from the scattering of the first coordination sphere of the iron. These filtered oscillations have been modeled[29] in terms of the six nitrogen near-neighbor scattering atoms, their distance to the central iron atom, and the iron Debye−Waller factor. The resulting best fit parameters are given in Table 5. All the adjustable parameters are reasonable, and specifically, the iron−nitrogen bond distances are in excellent agreement with the distances obtained from the single-crystal X-ray diffraction results given above.

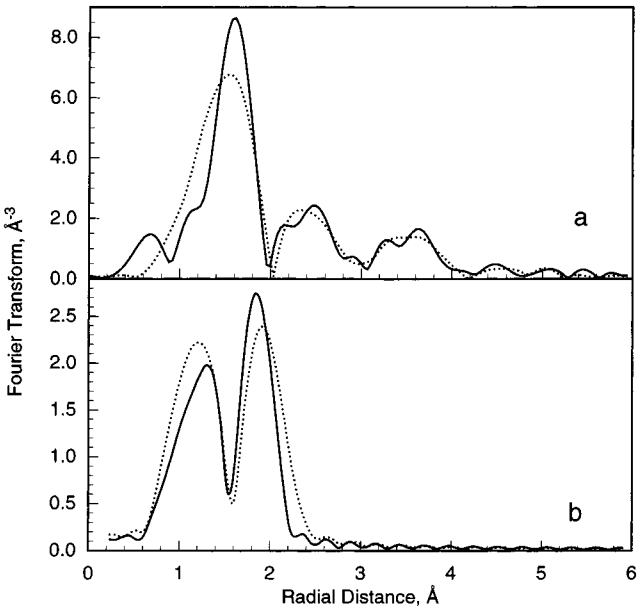

Figure 13. Fourier transforms (295 K) of the EXAFS oscillations for **1** (solid line) and **2** (dotted line) (a) and Fourier transforms (78 K) obtained for **1** (dotted line) and a simulation (solid line) with the parameters given in Table 5 (b).

Table 5. Analysis of the Iron K-Edge EXAFS Oscillations[a]

complex	*T*, K	no. of N nn[b]	Fe−N bond length, Å	σ, Å	Γ,[c] Å^{-2}	*R*,[d] %
1	295	6	2.17	0.075	1.25	0.01
	78	4	2.15	0.058	1.25	8.26
		2	1.96	0.050	1.20	
2	295	6	1.97	0.072	1.20	0.04
	78	6	1.97	0.066	1.20	0.10

[a] The bond lengths are accurate to ±0.01 Å, and the Debye−Waller factors, σ, are accurate to ±0.005 Å. [b] The number of nitrogen near neighbors of iron. [c] Γ is related to the electron mean free path by the relationship $\lambda(k) = k/\Gamma$. [d] *R* is the quality factor of the fit.

The analysis of the filtered oscillations at 78 K for **1** is not straightforward because of the presence of both iron(II) spin states. In an attempt to fit the oscillations shown by the dotted line in Figure 12b, a 50:50 linear combination of the 295 K oscillations for LS **2** and HS **1** have been calculated. A comparison between this linear combination and the experimental results, see Figure 12c, clearly indicates that a 50:50 mixture, as indicated by the magnetic and Mössbauer spectral results discussed above, is not adequate. Figure 12d shows the much more satisfactory agreement obtained between the experimental data and a 30:70 linear combination of the 295 K oscillations of LS **2** and HS **1**. Such a combination is also in relatively good agreement with the XANES results shown in Figure 11. The Fourier transform of the 78 K EXAFS oscillations for **1** shows two peaks which are associated, respectively, with the LS and HS components found at 78 K in **1**. This transform has been filtered and back-Fourier-transformed, and the resulting oscillation, shown in Figure 12e, has been satisfactorily simulated, see Figure 13b, with the parameters given in Table 5. In this case, the N near-neighbor values of 4 and 2 represent the fraction of HS and LS iron(II). Hence, the EXAFS results indicate that ca. 30% of **1** has been converted

(29) McKale, A. G.; Veal, B. W.; Paulikas, A. P.; Chan, S. K.; Knapp, G. S. *J. Am. Chem. Soc.* **1988**, *110*, 3763.

to the LS state at 78 K. If one tries to use the expected 3 and 3 ratio to represent the 50% HS to LS ratio, one obtains substantially poorer fits.

At this point it is not clear why the XANES and EXAFS studies of this compound seem to indicate a 30% LS:70% HS mixture rather than the expected 50:50 mixture of spin states at low temperature. The difference may be related to the preparation of the spectral absorber, which involved grinding **1** with cellulose and pressing the resulting mixture into a pellet at ca. 2000 psi. No such pressure was used to prepare the Mössbauer spectral absorbers. The application of such pressures is known to influence the spin crossover in iron(II) complexes.[1,2a] But a subsequent 78 K Mössbauer spectral study of exactly the same absorber used for the XANES and EXAFS studies gave results which were identical to the Mössbauer spectral results reported above. So perhaps the differences arise from the approximations involved in the EXAFS treatment presented herein. First, it is expected that the HS fraction contributes a more pronounced contribution to the EXAFS oscillations than the LS fraction. Second, to simulate the 78 K EXAFS oscillations for **1**, we use the EXAFS oscillations of **2**, a compound which does not contain the methyl groups, groups that may well contribute to the 78 K spectrum for **1**.

Conclusions

Structural, magnetic, and NMR, Mössbauer, and X-ray absorption spectral results for **1** indicate that the compound is HS at 298 K in both the solid phase and solution. The ambient-temperature crystal structure shows one unique iron(II) site. Below 206 K, crystalline **1** rapidly changes over to a 50:50 mixture of HS and LS states, a mixture that does *not continue to change its composition as the temperature is lowered* below 200 K. The crystalline sample also shows a slight irreversible increase in its magnetic moment below 85 K. After the slight irreversible change, crystals of **1** reversibly change from the HS state above 206 K to the 50:50 mixture below 200 K, showing no hysteresis upon cooling and heating. In contrast, **2** is LS at 298 K in the solid phase, changing over gradually to the HS state such that at ca. 470 K it is completely HS. In solution, both HS and LS forms of **2** are observed by ^{1}H NMR in the temperature range of 223−303 K, with the percentage of the HS form increasing as the temperature increases. The complex **3** is LS under all conditions studied.

Recent review articles and textbooks list five types of spin-crossover behavior.[1] The abrupt and reversible spin crossover of **1** below 206 K to yield a mixture of the HS and LS states, a mixture that does *not continue to change its composition as the temperature is lowered* below 200 K, is new for a complex that contains only one crystallographic iron site when fully HS and represents the sixth type of spin-crossover behavior.

Acknowledgment. Acknowledgment is made to the National Science Foundation (NSF) (Grants CHE-9727325 for D.L.R. and DMR-9521739 for G.J.L.) and the European Commission for Human Capital and Mobility (Contract ERBHXCT930360) for support. The NSF (Grants CHE-8904942 and CHE-9601723) and National Institutes of Health (NIH) (Grant RR-02425) have supplied funds to support the NMR equipment, and the NIH (Grant RR-02849) has supplied funds to support the mass spectrometry equipment at the University of South Carolina. We acknowledge, with thanks, the help of Mr. Jérôme Loicq and Mr. Faysal Bouamrame in obtaining the XANES and EXAFS data, and Professor Hanno zur Loye and Katharine Stitzer for assistance in obtaining the magnetic data. G.J.L. thanks the "Fonds National de la Recherche Scientifique" for support during a sabbatical leave in Belgium.

Supporting Information Available: Two X-ray crystallographic files for **2** and **3** in CIF format. This material is available free of charge via the Internet at http://pubs.acs.org.

IC001102T